Journal of Microbiology (2022) Vol. 60, No. 12, pp. 1162–1167
DOI 10.1007/s12275-022-2437-9
eISSN 1976-3794
pISSN 1225-8873

Transcript-specific selective translation by specialized ribosomes bearing genome-encoded heterogeneous rRNAs in *V. vulnificus* CMCP6

Younkyung Choi[1†], Minju Joo[1†], Wooseok Song[1†], Minho Lee[2], Hana Hyeon[1], Hyun-Lee Kim[1], Ji-Hyun Yeom[1], Kangseok Lee[1*], and Eunkyoung Shin[1*]

[1]*Department of Life Science, Chung-Ang University, Seoul 06974, Republic of Korea*
[2]*Department of Microbiology, College of Medicine, Hallym University, Chuncheon 24252, Republic of Korea*

(Received Sep 28, 2022 / Revised Oct 26, 2022 / Accepted Oct 27, 2022)

Ribosomes composed of genome-encoded heterogeneous rRNAs are implicated in the rapid adaptation of bacterial cells to environmental changes. A previous study showed that ribosomes bearing the most heterogeneous rRNAs expressed from the *rrnI* operon (I-ribosomes) are implicated in the preferential translation of a subset of mRNAs, including *hspA* and *tpiA*, in *Vibrio vulnificus* CMCP6. In this study, we show that HspA nascent peptides were predominantly bound to I-ribosomes. Specifically, I-ribosomes were enriched more than two-fold in ribosomes that were pulled down by immunoprecipitation of HspA peptides compared with the proportion of I-ribosomes in crude ribosomes and ribosomes pulled down by immunoprecipitation of RNA polymerase subunit ß peptides in the wild-type (WT) and *rrnI*-completed strains. Other methods that utilized the incorporation of an affinity tag in 23S rRNA or chimeric rRNA tethering 16S and 23S rRNAs, which generated specialized functional ribosomes in *Escherichia coli*, did not result in functional I-ribosomes in *V. vulnificus* CMCP6. This study provides direct evidence of the preferential translation of *hspA* mRNA by I-ribosomes.

Keywords: ribosome, heterogenous rRNAs, specialized ribosomes, *V. vulnificus* CMCP6, pathogenic bacteria

Introduction

Ribosomes are generally regarded as homogeneous molecular assemblies that passively contribute to gene expression rather than regulating gene expression (Brenner *et al.*, 1961). However, a large body of evidence shows ribosome heterogeneity (for a recent review, see [Genuth and Barna, 2018a, 2018b; Norris *et al.*, 2021; Barna *et al.*, 2022; Joo *et al.*, 2022]). This heterogeneity stems from the composition of rRNA, ribosomal proteins, ribosome-associated factors, or modifications to either set of components.

Ribosome heterogeneity originating from variant rRNAs has been observed in individual organisms in all three domains of life (Yagura *et al.*, 1979; Arnheim *et al.*, 1980; Gonzalez *et al.*, 1985; Maden *et al.*, 1987). For example, two distinct sets of rRNAs are expressed in malaria-causing *Plasmodium parasites* at different developmental stages, although their functional differences have not been identified (Gunderson *et al.*, 1987; Waters *et al.*, 1989; Velichutina *et al.*, 1998; van Spaendonk *et al.*, 2001). In halophilic archaea *Haloarcula* species, genome-encoded heterogeneous rRNAs are differentially expressed and are proposed to contribute to the rapid growth of these bacteria at high temperatures. A recent study showed that, in *Escherichia coli*, subpopulations of ribosomes containing variant rRNAs affected the expression of stress response genes via an unknown mechanism (Kurylo *et al.*, 2018).

It has also been reported that MazF and RNase G, endoribonucleases, participate in the generation of heterogeneous rRNAs and, consequently, subpopulations of variant ribosomes in *E. coli* that have specialized functions (Tock *et al.*, 2000; Zhang *et al.*, 2004; Song *et al.*, 2014). Although ribosome heterogeneity by variant rRNAs has been recognized, their physiological roles remain largely unknown.

Recently, our research group has shown that *V. vulnificus* CMCP6 produced a subpopulation of ribosomes containing the most variable rRNAs (I-ribosome) that directed the preferential translation of a subset of mRNAs that included *hspA* and *tpiA* (Song *et al.*, 2019). This phenomenon enabled bacterial cells to rapidly adapt to environmental changes, such as nutrient and temperature shifts.

We further investigated the molecular mechanism underlying the transcript-specific selective translation of I-ribosome. This study presents results from the construction and characterization of specialized I-ribosomes containing rRNA with an affinity tag or chimeric rRNAs. This study also presents evidence for the preferential translation of *hspA* mRNA by I-ribosomes using immunoprecipitation of nascent HspA.

Materials and Methods

Bacterial strains and plasmid construction

Vibrio vulnificus CMCP6 strains were grown at 30°C in LBS media. The bacterial strains, plasmids, and primers used in this study are listed in Tables 1 and 2. Plasmid constructs were conjugated into *V. vulnificus* CMCP6.

An MS2-tag was chosen as the affinity tag to construct

†These authors contributed equally to this work.
*For correspondence. (K. Lee) E-mail: kangseok@cau.ac.kr / (E. Shin) E-mail: stella0608@cau.ac.kr

Table 1. Bacterial strains or plasmids used in this study

Strains or plasmids	Relevant characteristics	References
Vibrio vulnificus		
CMCP6	Clinical isolate	Song *et al.* (2019)
Δ*rrnI*	Same as CMCP6 but *rrnI*::Km^R	Song *et al.* (2019)
Plasmids		
pRK415	RK2-derived *oriV*, Tn^R	Keen *et al.* (1988)
pRK415-*rrnI*	pRK415 containing the *rrnI* operon	Song *et al.* (2019)
pRK415-*rrnI*-Δ23S	pRK415 lacking 23S rRNA gene	In this study
pRK415-*rrnI*^{MS2}	pRK415 containing the MS2 tagged-*rrnI* operon	In this study
pRK415-*rrnI*^{tether}	pRK415 containing the tethered *rrnI* operon	In this study

pRK415-*rrnI*^{MS2}, as previously described (Youngman and Green, 2005). Briefly, the loop of interest (MS2-tag) was amplified using *V. vulnificus* CMCP6 genomic DNA as a template and assembled by overlap extension polymerase chain reaction (PCR) using the primer pairs *rrnI*-23S-2534F and 23S-MS2-R and 23S-MS2-F and *rrnI*-PstI-R (Table 2). The amplified fragments were ligated into the ClaI/PstI sites of pRK415, which carries the *V. vulnificus* CMCP6 *rrnI* operon, as previously described (LeCuyer *et al.*, 1995).

The Ribo-T-based approach was utilized to construct pRK-415-*rrnI*^{tether}, as previously described (Orelle *et al.*, 2015). The pRK415-*rrnI* plasmid lacking the 23S rRNA gene (pRK415-*rrnI*-Δ23S), used for cloning the tethered *rrnI* gene, was prepared using a PCR-based site-directed mutagenesis method. The 16S- and 23S-I-rRNA regions were PCR-amplified from the pRK415-*rrnI* plasmid and assembled by serial overlap extension PCR using the appropriate primer pairs listed in Table 2. The H101 regions of the 23S rRNA gene were linked with the h44 region of the 16S rRNA gene through the two linkers and connectors. The amplified fragments were ligated into the BglII/XbaI sites of the pRK415-*rrnI*-Δ23S plasmid. The construction of pRK415-*rrnI*^{tether} was confirmed by double digestion with EcoRI and PstI and by sequencing.

Table 2. Primers used in this study

Primers	Sequence (5′ – 3′)
Construction of pRK415-*rrnI*$^{comp-MS2}$	
23S-2534F	AGGGTATGGCTGTTCGCCAT
23S-MS2-F	GATGAGTCTTCCCTGATACTTGATCATTTCTACACATTAGTAGTAGTTTTGATCA
23S-MS2-R	GAACAACCCTTCAGGATACTTGATCAAAACTACTACTAATGTGTAGAAATGATCA
rrnI PstI-R	ATCTGCAGCGGAGAGATAGGGATTTG
Construction of pRK415-*rrnI*$^{comp-tether}$	
I-tether P1	ATGCGTAGAGATCTGAAGGA
I-tether P2	TTTTTTTTAGGTTAAACTACCCACTTCTTTTG
I-tether P3	CAAAAGAAGTGGGTAGTTTAACCTAAAAAAAAGAGGCGTTGAGCTAACCTGTACTA
I-tether P4	ATTCTAGAATGGTTAAGCCTCACGGGCAA
I-tether P5	TCTCATGGTTAAGCCTCACGGGCAA
I-tether P6	TTGCCCGTGAGGCTTAACCATGAGAATGGTTAAGTGACTAAGCGTA
I-tether P7	CTTCCGCGCAGGCCGACTCG
I-tether P8	CGTAATAGCTCACTAGTCGA
I-tether P9	TTTTTTTTTACAGCGCTTACACACCCTGC
I-tether P10	GGGTGTGTAAGCGCTGT AAAAAAAAA TCGGGAGGACGCTCACCACTTTG
I-tether P11	TGTCCTAGGCCTCTAGACGA
oriT R(EcoRI)	ATGAATTCCGTCGGTGATGTACTTCACCA
oriT F(SalI)	ATGTCGACGCGTGGCGCTTTTCCGCTGCA
rrnI 23S 5′end R	CTTTGGGTGTTGTATATACAACCCCAAAGGGTCTTTGTTA
rrnI 23S 3'end F	GGGTTGTATATACAACACCCAAAGGGTTTTGATGGA
rrnI 23S 3'end R	ATGAGCTCAAAAACTAGTGCATGCCTGCAGCGGAGAGATA
For allele-specific RT-PCR	
23S-1148 rRNA-F	TGCGGCAATGTTCTTTGAAC
23S-1148 I-rRNA-F	TGCGGCAATATCTTTTAGAT
23S-rRNA-1350R	CGGCCTCGCCTTAGGGGTCG
For RT-PCR	
23S-2534F	AGGGTATGGCTGTTCGCCAT
23S-2833R	TGCCTATCAACGTTCTAGTC
16S-1390F	GGCTTGTACACACCGCCCG
23S-60R	TTCATCGCCTCTGACTGCCA

Isolation of total RNA and crude ribosomes

Total RNA and crude ribosomes were isolated as previously described (Song *et al.*, 2019). Cells were grown to mid-log phase at 30°C in LBS media containing 0.2 μg/ml tetracycline. The quality and quantity of the extracted crude ribosomes were assessed using a Nanodrop 2000 instrument (Thermo Fischer Scientific).

Reverse transcription PCR (RT-PCR) analysis

Samples for reverse transcription (RT)-PCR were prepared and analyzed as previously described (Lee *et al.*, 2019). The tagged-rRNA's complementary DNA (cDNA) was synthesized from total RNA or crude ribosomes from Δ*rrnI*, Δ*rrnI*^{comp}, or Δ*rrnI*$^{comp\text{-}MS2}$ cells, and amplified using primers 23S-2534F and 23S-2833R. The tethered-rRNA's cDNA was synthesized from crude ribosomes from Δ*rrnI*, Δ*rrnI*^{comp}, or Δ*rrnI*$^{comp\text{-}tether}$ cells, and amplified using primers 16S-1390F and 23S-60R. PCR products were electrophoresed on a 1.5% agarose gel containing ethidium bromide.

Quantification of I-rRNA distribution.

The distribution of I-rRNAs in ribosomes was determined by allele-specific RT-PCR, as previously described (Song *et al.*, 2019). Briefly, rRNAs were purified from crude ribosomes by phenol-chloroform extraction followed by ethanol precipitation (Patel, 2001). For the amplification of I-rRNAs for allele-specific RT-PCR, cDNA was synthesized using PrimeScript™ 1st strand cDNA Synthesis Kit (TaKaRa Bio Inc.) according to the manufacturer's instructions. Primers specific for 23S *rrnI* were designed with a mismatch at the variable nucleotide position. PCR cycling was performed using the following parameters: an initial denaturation step at 95°C for 3 min; then 32 cycles at 95°C for 30 sec, 65°C for 30 sec, and 72°C for 20 sec; and a final extension step at 72°C for 3 min. PCR products were separated on a 2% agarose gel by electrophoresis and visualized under ultraviolet light.

Western blot analysis

Proteins were resolved on 12% sodium dodecyl sulfate-polyacrylamide gels. The gels were electroblotted onto nitrocellulose membranes. Images of the western blots were obtained using an Amersham Imager 600 (GE Healthcare Life Sciences) and were quantified using Quantity One (Bio-Rad Laboratories). The ribosomal protein S1 was used as the control. The following antibodies were used in this study: anti-HspA (generated in our laboratory [Song *et al.*, 2019]), anti-RNAP-β (Abcam), and anti-S1 (obtained from Dr. Stanley N. Cohen's laboratory [Song *et al.*, 2019]).

Co-immunoprecipitation

Co-immunoprecipitation of nascent peptides of HspA or RNAP-β subunit bound ribosomes was performed using Dynabeads Protein G (Invitrogen). Before binding the magnetic beads with anti-HspA or anti-RNAP-β subunit antibodies, 1 pmole of crude ribosomes and 30 μl of antibodies were added to buffer B with 0.05% Tween-20 and rotated overnight at 4°C. This mixture was combined with 0.9 mg of magnetic beads that were washed with Buffer B containing 0.05% Tween-20 and incubated for three hours using a rotator. The beads were washed with 1× bind and wash (B&W) buffer (5 mM pH 7.5 Tris-HCl + 0.5 mM EDTA + 1 M NaCl) and eluted using elution buffer (95% formamide + 10 mM EDTA, pH 8.2) for 10 min at 65°C. The eluted samples were confirmed by western blot, and total RNA was purified by ethanol precipitation. Purified RNA samples were quantified by allele-specific RT-PCR.

Statistical analysis

All statistical details of experiments are included in the Figure legends. Multiple-comparison analyses of values were performed using the Student–Newman–Keuls test, and Student's *t*-test was used for comparisons with control samples, using SAS version 9.4 (SAS Institute) and SigmaPlot (Systat Software) (Na, 2020). The data are presented as the mean ± stan-

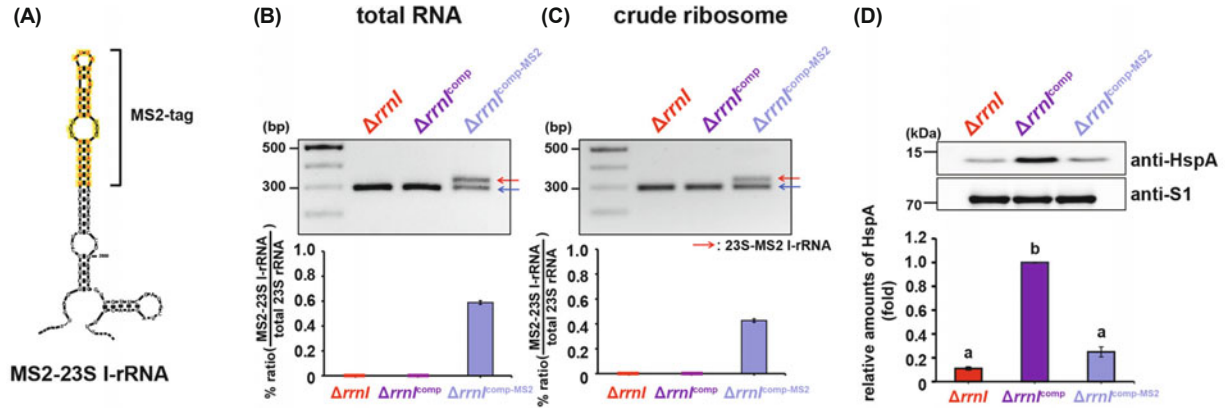

Fig. 1. Construction of affinity tagged ribosome for expressing MS2-tagged 23S I-rRNA. (A) A schematic representation of the insertion sites of the MS2-tag. The MS2 RNA aptamer sequences are highlighted in yellow. (B and C) The analysis of MS2-tagged I-rRNAs expression and assembly in Δ*rrnI* cells harboring pRK415-*rrnI* (Δ*rrnI*^{comp}) and pRK415-*rrnI*-23SMS2 (Δ*rrnI*$^{comp\text{-}MS2}$) using RT-PCR with primers, 23S-2534F and 23S-2833R. The cDNA was synthesized from the total RNA (B) or crude ribosomes (C) of these strains. The PCR products were resolved in a 1.5% agarose gel. Each group's relative abundance was quantitated and is shown at the bottom of the gel. Red arrows indicate the MS2-tagged rRNAs. Blue arrows indicate the 23S rRNAs encoded by other *rrn* operons. (D) Effects of MS2-tagged ribosome on the synthesis of HspA. The expression levels of HspA were compared by setting the expression of Δ*rrnI*^{comp} to one. The data are presented as the mean ± *SEM*, and significant differences are indicated with letters ($p < 0.0001$).

dard error of the mean (*SEM*); a *p*-value of less than 0.05 was considered statistically significant.

Results

Effect of MS2-tagged-I-ribosome on *hspA* expression of *V. vulnificus* CMCP6

The affinity tagged-ribosome purification system developed by Dr. Rachel Green's group was used to affinity-purify I-ribosomes (Youngman and Green, 2005). This method uses a well-characterized aptamer from the MS2 phage (MS2-tag), which can bind the MS2 coat-glutathione S-transferase (GST) fusion protein as an affinity tag to purify mutated *E. coli* ribosomes. An MS2-tagged-*rrnI*-complemented (Δ*rrnI* + pRK415-MS2-*rrnI*; Δ*rrnI*$^{comp\text{-}MS2}$) *V. vulnificus* CMCP6 strain was constructed and characterized. The sequence and secondary structure of the MS2-tagged 23S I-rRNA (MS2-23S I-rRNAs) construct are illustrated in Fig. 1A. A 16S I-rRNAs containing the MS2-aptamer was not created because the 16S rRNA insertion site in *V. vulnificus* was close to the region clustered with variable residues implicated in I-ribosome function (Song *et al*., 2019). The incorporation of exogenously expressed MS2-tagged I-rRNAs into ribosomes was assessed by RT-PCR (Fig. 1B and C). The MS2-23S I-rRNAs from the variant *rrnI* operon (*rrnI*^{MS2}) represented about 60% of the total RNA in the Δ*rrnI*$^{comp\text{-}MS2}$ strains and about 40% of the WT-23S I-rRNAs from the crude ribosomes in the Δ*rrnI*$^{comp\text{-}MS2}$ strains, respectively (Fig. 1B and C). In addition, *rrnI*-deleted (Δ*rrnI* + pRK415; Δ*rrnI*) and *rrnI*-complemented (Δ*rrnI* + pRK415-*rrnI*; Δ*rrnI*^{comp}) strains were used as controls to assess the function of ribosomes bearing MS2-tagged I-rRNAs in *V. vulnificus* CMCP6.

Whether the presence of the 23S-MS2 tag interfered with I-ribosome function *in vivo* was investigated by assessing the expression levels of the HspA protein in Δ*rrnI*$^{comp\text{-}MS2}$ cells. As shown in Fig. 1D, there was a modest increase (about 2-fold) in HspA protein levels in the Δ*rrnI*$^{comp\text{-}MS2}$ strain compared with the levels in the Δ*rrnI* strain (Fig. 1D). HspA expression was increased about 10-fold in the Δ*rrnI*^{comp} strain compared with the levels in Δ*rrnI* strain (Fig. 1D), similar to previously reported results. (Song *et al*., 2019). These results suggest that I-ribosomes bearing the MS2-tag in the 23S I-rRNAs mostly lost the ability to preferentially translate *hspA* mRNA in *V. vulnificus* CMPC6.

Effect of tethered I-ribosome on *hspA* expression of *V. vulnificus* CMCP6

A previous study showed that engineered ribosomes whose small and large subunits were tethered together by the linkage of 16S- and 23S-rRNAs were functional and supported normal cellular growth in *E. coli* (Orelle *et al*., 2015). Since these tethered ribosomes have a distinct sedimentation coefficient in a sucrose gradient centrifugation, they can be purified for biochemical analyses. In addition, this system can be used to further investigate the previous finding showing that the expression of 16S I-rRNA and 23S-5S I-rRNA are required for the enhanced expression of HspA (Song *et al*., 2019). For these reasons, an engineered I-ribosomes with its small and large subunits tethered together by linking the 16S- and 23S-rRNAs was constructed in *V. vulnificus* CMCP6. The small and large subunits were tethered together via helix 44 (h44) of the 16S I-rRNA and helix 101 (H101) of the 23S I-rRNA, which generated the chimeric 16S–23S I-rRNA molecule, as previously described (Orelle *et al*., 2015) (Fig. 2A). The expression and incorporation of the tethered I-rRNAs into ribosomes were assessed by analyzing the amounts of tethered-I-rRNA in the crude ribosome samples using RT-PCR with tether-site specific primers. The results showed distinct cDNA products from the tethered I-rRNA from the crude ribosomes in the Δ*rrnI* strain expressing the tethered I-rRNA (Δ*rrnI*$^{comp\text{-}tether}$) (Fig. 2B).

The tethered I-ribosomes were then tested for functionality by analyzing the effect of the tethered I-ribosome on HspA protein synthesis. The expression of the tethered I-ribosomes did not result in enhanced expression of HspA in Δ*rrnI*$^{comp\text{-}tether}$ cells compared with the HspA levels in Δ*rrnI* cells (Fig. 2C). These results suggest that chimeric rRNA

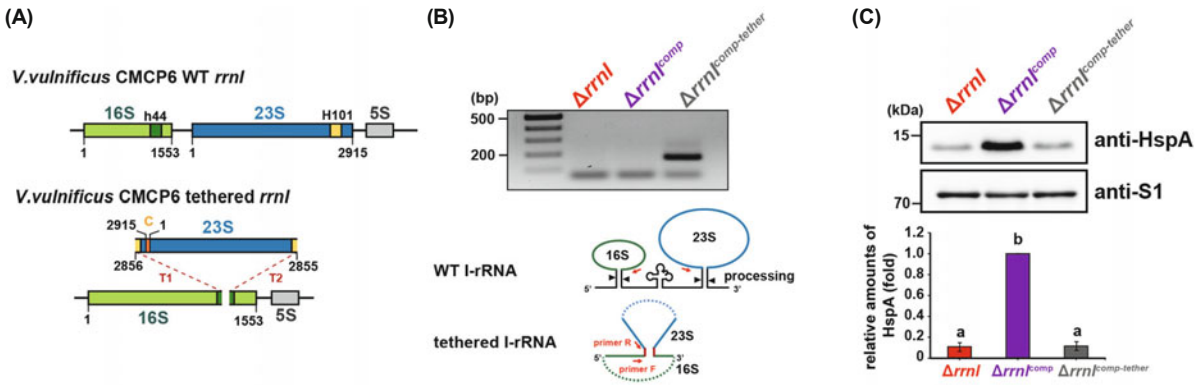

Fig. 2. Construction of I-ribosomes with tethered subunits in *V. vulnificus* CMCP6. (A) An experimental scheme for constructing the chimeric 16S–23S I-rRNA operon. In tethered ribosomes, the loop of H101 in the 23S I-rRNA gene has a four-nucleotide long connector (C) is linked to the apex loop of h44 in the 16S rRNA gene via the tether T1 (A_8) and T2 (A_9). (B) The analysis of tethered-I-rRNAs expression and incorporation into ribosomes using RT-PCR with tether-site specific primers (16S-1390F and 23S-60R). The cDNA was synthesized from the crude ribosome samples from WT, Δ*rrnI*, or Δ*rrnI*$^{comp\text{-}tether}$ strains. The PCR products were resolved in a 1.5% agarose gel. The primers are indicated by arrows. (C) The effects of the tethered ribosomes on the synthesis of HspA. The expression levels of HspA were compared by setting the expression level of Δ*rrnI*^{comp} to one. The data are presented as the mean ± *SEM*, and significant differences are indicated with letters ($p < 0.0001$).

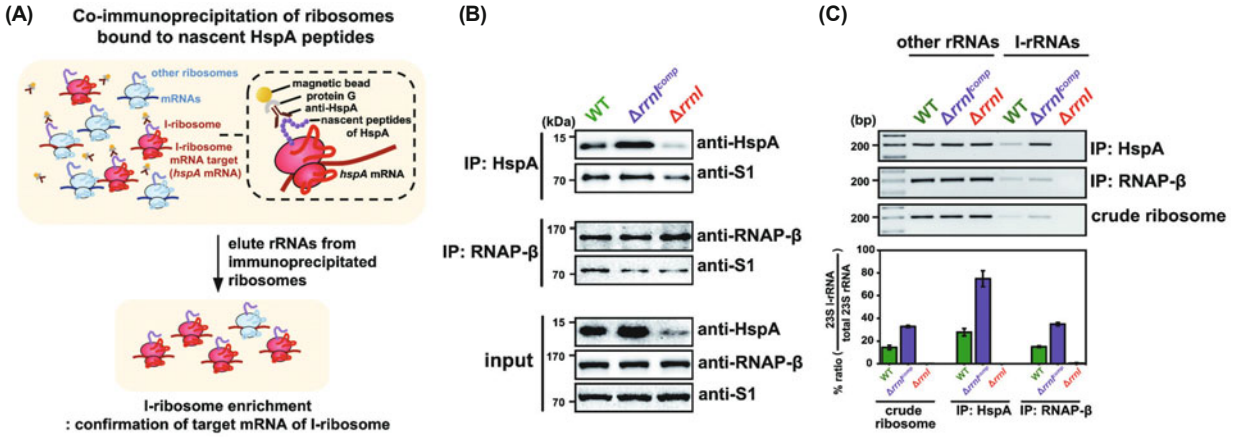

Fig. 3. Co-immunoprecipitation assays showing predominant interactions of I-ribosomes with HspA nascent peptides. (A) A schematic of the procedure of co-IP analysis of the nascent peptides bound ribosomes. (1) Crude ribosomes were isolated from *V. vulnificus* CMCP6 WT, Δ*rrnI*, or Δ*rrnI*^{comp} cell lysates. (2) Isolated crude ribosomes were incubated with anti-HspA or anti-RNAP-β antibodies. (3) Nascent peptides bound to ribosomes were immunoprecipitated using protein G magnetic beads. Beads were separated from the precipitated samples using a magnet. (4) rRNAs were purified from immunoprecipitated ribosomes or crude ribosomes (Input). The relative amounts of I-ribosomes were analyzed by allele-specific RT-PCR using common and I-rRNA-specific primers listed in Table 2. (B) The identification of HspA and the RNAP-β subunit after co-IP. The precipitate was subjected to western blotting using antibodies against HspA or RNAP-β. The S1 protein was used as a loading control. (C) The characterization of the expression and assembly of I-rRNAs after co-IP. The number of amplicons of 23S I-rRNAs and other 23S rRNAs amplified from the cDNAs of the WT, Δ*rrnI*, or Δ*rrnI*^{comp} strains was determined by PCR using common and allele-specific primers. The cDNA was synthesized from rRNAs purified from immunoprecipitated samples or crude ribosome samples, which was used as a control. The PCR products were resolved in a 2% agarose gel. The data are presented as the mean ± *SEM* of three independent experiments.

tethering of 16S and 23S rRNAs, generated specialized functional ribosomes in *E. coli* and did not constitute functional I-ribosomes in *V. vulnificus* CMCP6.

Preferential association of nascent HspA peptides to I-ribosome

Whether the enhanced translation of *hspA* mRNA in Δ*rrnI*^{comp} cells was a direct consequence of the preferential binding of I-ribosome to *hspA* mRNA was investigated by a co-immunoprecipitation analysis using anti-HspA antibodies. The co-immunoprecipitation analysis tested the direct molecular interactions between I-ribosomes and HspA nascent peptides *in vivo*. A schematic outline of the immunoprecipitation procedure used in this study is shown in Fig. 3A. First, nascent HspA-bound ribosomes were pulled down from the crude ribosomes isolated from WT, Δ*rrnI*, or Δ*rrnI*^{comp} *V. vulnificus* CMCP6 cells using anti-HspA antibodies. The samples were immunoprecipitated using protein G magnetic beads. The co-immunoprecipitation (co-IP) of the RNA Polymerase subunit β subunit (RNAP-β) was also included and used as a control for non-preferential translation of I-ribosome. Western blot analysis of the immunoprecipitated fraction from the nascent HspA-bound ribosomes revealed that HspA proteins were highly enriched in the Δ*rrnI*^{comp} strain compared with those of the WT or Δ*rrnI* strains (Fig. 3B). In contrast, no significant changes in RNAP-β expressions were detected in any of the strains used in these experiments (Fig. 3B).

Total rRNA was purified from the crude ribosomes and immunoprecipitated ribosomes (nascent-HspA or RNAP-β subunit-bound ribosomes), and the distribution and incorporation of the I-rRNAs were measured by allele-specific RT-PCR. I-rRNAs accounted for about 15% of the total rRNAs from crude ribosome samples from the WT strain and about 33% of the total rRNAs from crude ribosome samples from the Δ*rrnI*^{comp} strain (Fig. 3C). In contrast, 23S rRNAs form the *rrnI* operon represented about 35% of the total rRNAs from HspA-bound ribosomes in the WT strain and about 75% of the total rRNAs from HspA-bound ribosomes in the Δ*rrnI*^{comp} strain. The proportion of I-rRNAs from RNAP-β-bound ribosomes was similar to that found in the crude ribosomes from the WT and Δ*rrnI*^{comp} strains (Fig. 3C). Thus, these results provide direct evidence showing the preferential binding and translation of *hspA* mRNA by I-ribosome in *V. vulnificus* CMCP6.

Discussion

One of the critical questions raised by the observations of heterogeneity in ribosome composition, including variations of rRNA, is what their physiological functions are. We previously reported that ribosomes harboring genome-encoded divergent rRNAs expressed from the *rrn*I operon preferentially translated a subset of mRNAs, including *hspA* and *tpiA*, in *V. vulnificus* CMCP6 (Song *et al.*, 2019). This study aimed to obtain direct evidence for the preferential binding of *hspA* mRNA by I-ribosomes in *V. vulnificus* CMCP6. We show that HspA nascent peptides were predominantly bound to I-ribosomes by analyzing co-immunoprecipitated ribosomes with HspA peptides (Fig. 3).

We wished to purify I-ribosomes for biochemical analyses to analyze the molecular mechanisms underlying the ability of I-ribosome to selectively bind and translate specific mRNAs. For this purpose, we employed two methods, the incorporation of an aptamer to MS2 affinity tag in 23S I-rRNA (Fig.

1) and the creation of tethered I-rRNAs (Fig. 2). However, these I-rRNAs modifications resulted in the loss of I-ribosome function in enhanced HspA expression in *V. vulnificus* CMCP6 (Figs. 1D and 2C). Based on the results showing that these modified I-rRNAs were assembled in the ribosomes (Figs. 1C and 2B) and that these modifications did not affect the function of ribosomes in *E. coli* (Youngman and Green, 2005; Orelle *et al*., 2015), we speculate that these modifications might abolish the ability of I-ribosomes to preferentially translate *hspA* mRNA while maintaining normal protein synthesis. However, further studies are needed to understand how these modifications lead to the loss of I-ribosome function in preferential *hspA* mRNA translation.

In conclusion, this study provides direct evidence for the preferential binding of nascent HspA peptides to I-ribosome, indicating that the enhanced translation of *hspA* mRNAs is proportional to I-ribosome abundance in *V. vulnificus* CMCP6 and is a direct consequence of the preferential translation of *hspA* mRNA by I-ribosomes. Although identifying the detailed molecular mechanisms and physiological functions of heterogeneous ribosomes remain a major challenge, this study provides evidence of the specialized functions of ribosomes bearing genome-encoded heterogeneous rRNAs.

Acknowledgements

This research was supported by the Chung-Ang University Graduate Research Scholarship grants in 2020 and the National Research Foundation of Korea [NRF-2021R1A2C3-008934 to K. L. and NRF-2021R1I1A1A01058183 to E. S].

Conflict of Interest

The authors declare that they have no conflicts of interest.

References

Arnheim, N., Krystal, M., Schmickel, R., Wilson, G., Ryder, O., and Zimmer, E. 1980. Molecular evidence for genetic exchanges among ribosomal genes on nonhomologous chromosomes in man and apes. *Proc. Natl. Acad. Sci. USA* **77**, 7323–7327.

Barna, M., Karbstein, K., Tollervey, D., Ruggero, D., Brar, G., Greer, E.L., and Dinman, J.D. 2022. The promises and pitfalls of specialized ribosomes. *Mol. Cell* **82**, 2179–2184.

Brenner, S., Jacob, F., and Meselson, M. 1961. An unstable intermediate carrying information from genes to ribosomes for protein synthesis. *Nature* **190**, 576–581.

Genuth, N.R. and Barna, M. 2018a. Heterogeneity and specialized functions of translation machinery: from genes to organisms. *Nat. Rev. Genet.* **19**, 431–452.

Genuth, N.R. and Barna, M. 2018b. The discovery of ribosome heterogeneity and its implications for gene regulation and organismal life. *Mol. Cell* **71**, 364–374.

Gonzalez, I.L., Gorski, J.L., Campen, T.J., Dorney, D.J., Erickson, J.M., Sylvester, J.E., and Schmickel, R.D. 1985. Variation among human 28S ribosomal RNA genes. *Proc. Natl. Acad. Sci. USA* **82**, 7666–7670.

Gunderson, J.H., Sogin, M.L., Wollett, G., Hollingdale, M., de la Cruz, V.F., Waters, A.P., and McCutchan, T.F. 1987. Structurally distinct, stage-specific ribosomes occur in *Plasmodium*. *Science* **238**, 933–937.

Joo, M., Yeom, J. H., Choi, Y., Jun, H., Song, W., Kim, H.L., Lee, K., and Shin, E. 2022. Specialised ribosomes as versatile regulators of gene expression. *RNA Biol.* **19**, 1103–1114.

Keen, N.T., Tamaki, S., Kobayashi, D., and Trollinger, D. 1988. Improved broad-host-range plasmids for DNA cloning in Gram-negative bacteria. *Gene* **70**, 191–197.

Kurylo, C.M., Parks, M.M., Juette, M.F., Zinshteyn, B., Altman, R.B., Thibado, J.K., Vincent, C.T., and Blanchard, S.C. 2018. Endogenous rRNA sequence variation can regulate stress response gene expression and phenotype. *Cell Rep.* **25**, 236–248.

LeCuyer, K.A., Behlen, L.S., and Uhlenbeck, O.C. 1995. Mutants of the bacteriophage MS2 coat protein that alter its cooperative binding to RNA. *Biochemistry* **34**, 10600–10606.

Lee, J., Lee, D.H., Jeon, C.O., and Lee, K. 2019. RNase G controls *tpi*A mRNA abundance in response to oxygen availability in *Escherichia coli*. *J. Microbiol.* **57**, 910–917.

Maden, B.E., Dent, C.L., Farrell, T.E., Garde, J., McCallum, F.S., and Wakeman, J.A. 1987. Clones of human ribosomal DNA containing the complete 18S-rRNA and 28S-rRNA genes. Characterization, a detailed map of the human ribosomal transcription unit and diversity among clones. *Biochem. J.* **246**, 519–527.

Na, D. 2020. User guides for biologists to learn computational methods. *J. Microbiol.* **58**, 173–175.

Norris, K., Hopes, T., and Aspden, J.L. 2021. Ribosome heterogeneity and specialization in development. *Wiley Interdiscip. Rev. RNA* **12**, e1644.

Orelle, C., Carlson, E.D., Szal, T., Florin, T., Jewett, M.C., and Mankin, A.S. 2015. Protein synthesis by ribosomes with tethered subunits. *Nature* **524**, 119–124.

Patel, J.B. 2001. 16S rRNA gene sequencing for bacterial pathogen identification in the clinical laboratory. *Mol. Diagn.* **6**, 313–321.

Song, W., Joo, M., Yeom, J.H., Shin, E., Lee, M., Choi, H.K., Hwang, J., Kim, Y.I., Seo, R., Lee, J.E., *et al.* 2019. Divergent rrnas as regulators of gene expression at the ribosome level. *Nat. Microbiol.* **4**, 515–526.

Song, W., Kim, Y.H., Sim, S.H., Hwang, S., Lee, J.H., Lee, Y., Bae, J., Hwang, J., and Lee, K. 2014. Antibiotic stress-induced modulation of the endoribonucleolytic activity of RNase III and RNase G confers resistance to aminoglycoside antibiotics in *Escherichia coli*. *Nucleic Acids Res.* **42**, 4669–4681.

Tock, M.R., Walsh, A.P., Carroll, G., and McDowall, K.J. 2000. The CafA protein required for the 5′-maturation of 16S rRNA is a 5′-end-dependent ribonuclease that has context-dependent broad sequence specificity. *J. Biol. Chem.* **275**, 8726–8732.

van Spaendonk, R.M., Ramesar, J., van Wigcheren, A., Eling, W., Beetsma, A.L., van Gemert, G.J., Hooghof, J., Janse, C.J., and Waters, A.P. 2001. Functional equivalence of structurally distinct ribosomes in the malaria parasite, *Plasmodium berghei*. *J. Biol. Chem.* **276**, 22638–22647.

Velichutina, I.V., Rogers, M.J., McCutchan, T.F., and Liebman, S.W. 1998. Chimeric rRNAs containing the GTPase centers of the developmentally regulated ribosomal rrnas of *Plasmodium falciparum* are functionally distinct. *RNA* **4**, 594–602.

Waters, A.P., Syin, C., and McCutchan, T.F. 1989. Developmental regulation of stage-specific ribosome populations in *Plasmodium*. *Nature* **342**, 438–440.

Yagura, T., Yagura, M., and Muramatsu, M. 1979. *Drosophila melanogaster* has different ribosomal RNA sequences on X and Y chromosomes. *J. Mol. Biol.* **133**, 533–547.

Youngman, E.M. and Green, R. 2005. Affinity purification of *in vivo*-assembled ribosomes for *in vitro* biochemical analysis. *Methods* **36**, 305–312.

Zhang, J., Zhang, Y., Zhu, L., Suzuki, M., and Inouye, M. 2004. Interference of mRNA function by sequence-specific endoribonuclease PemK. *J. Biol. Chem.* **279**, 20678–20684.